

# Single-shot mega-electronvolt ultrafast electron diffraction for structure dynamic studies of warm dense matter

M. Z. Mo,<sup>1,a)</sup> X. Shen,<sup>1</sup> Z. Chen,<sup>1</sup> R. K. Li,<sup>1</sup> M. Dunning,<sup>1</sup> K. Sokolowski-Tinten,<sup>2</sup> Q. Zheng,<sup>1</sup> S. P. Weathersby,<sup>1</sup> A. H. Reid,<sup>1</sup> R. Coffee,<sup>1</sup> I. Makasyuk,<sup>1</sup> S. Edstrom,<sup>1</sup> D. McCormick,<sup>1</sup> K. Jobe,<sup>1</sup> C. Hast,<sup>1</sup> S. H. Glenzer,<sup>1</sup> and X. Wang<sup>1</sup>

<sup>1</sup>SLAC National Accelerator Laboratory, 2575 Sand Hill Road, Menlo Park, California 94025, USA

<sup>2</sup>Faculty of Physics and Centre for Nanointegration Duisburg-Essen, University of Duisburg-Essen, Lotharstrasse 1, D-47048 Duisburg, Germany

(Presented 7 June 2016; received 9 June 2016; accepted 8 July 2016; published online 4 August 2016)

We have developed a single-shot mega-electronvolt ultrafast-electron-diffraction system to measure the structural dynamics of warm dense matter. The electron probe in this system is featured by a kinetic energy of 3.2 MeV and a total charge of 20 fC, with the FWHM pulse duration and spot size at sample of 350 fs and 120  $\mu$ m respectively. We demonstrate its unique capability by visualizing the atomic structural changes of warm dense gold formed from a laser-excited 35-nm freestanding single-crystal gold foil. The temporal evolution of the Bragg peak intensity and of the liquid signal during solid-liquid phase transition are quantitatively determined. This experimental capability opens up an exciting opportunity to unravel the atomic dynamics of structural phase transitions in warm dense matter regime. *Published by AIP Publishing.* [<http://dx.doi.org/10.1063/1.4960070>]

## I. INTRODUCTION

There is a significant interest in studies of warm dense matter (WDM)<sup>1</sup> and the phase transitions that lead to this regime. WDM state is found in steady state conditions in the interiors of large planets<sup>2</sup> and brown dwarfs<sup>3</sup> and is the precursor in the formation of high-density plasmas, especially in inertial confinement fusion (ICF) research.<sup>4</sup>

Experimentally, measuring the structural changes during solid/liquid phase transitions under WDM conditions is nontrivial due to their rapid evolution and the disorder of the ensuing structure. However, the recent advances in ultrafast diffraction techniques based on X-rays<sup>5</sup> and electrons<sup>5,6</sup> offer a great opportunity to help resolve this challenge. Electrons have a much larger ( $10^4$ – $10^6$  times) scattering cross sections than X-rays, making them the ideal choice to study nanometer-scale or thinner samples. Furthermore, the elastic mean-free-path of electrons is better matched to the optical pump excitation depth, which can further enhance their efficiency in the studies of laser-induced phase transitions.<sup>7</sup>

Recently, a mega-electronvolt ultrafast-electron-diffraction (MeV-UED) apparatus has been developed at SLAC's Accelerator Structure Test Area (ASTA) facility to support ultrafast science programs.<sup>8</sup> By using relativistic electrons, the inherent space charge effect, which tends to broaden the bunch, is significantly suppressed. Therefore high bunch charge and femtosecond temporal resolution become feasible for this technique. To serve the WDM physics studies, a single-shot data acquisition module has been added into this MeV-UED system since irreversible physical processes are normally

involved in a WDM system. In this paper, we report the characterization results of this single-shot MeV-UED system as well as its application to probe the structural phase transitions of WDM created by ultrafast optical excitation.

## II. EXPERIMENTAL SETUP

The details of the MeV-UED system in ASTA at SLAC have been described elsewhere.<sup>8</sup> The system can operate at a repetition rate up to 180 Hz and consists of the following key components: a Linac Coherent Light Source (LCLS)-type photocathode rf gun,<sup>9</sup> an ultra-stable rf power source, a laser-rf timing system, a Ti:sapphire laser system, and a phosphor screen-based electron detector. The rf gun is powered by a pulse-forming-network based modulator and a 50 MW S-band klystron. The rf signal in the gun is monitored by a phase and amplitude detector unit.<sup>10</sup> The stability of the rf phase and amplitude is maintained by a feedback loop that is based on a phase and amplitude controller unit.<sup>11</sup> Typical values of the rf amplitude and phase stability of the gun fields were measured to be  $3 \times 10^{-4}$  (rms) and 30 fs (rms) over hours. The timing jitter between the optical pump laser and the electron probe was controlled to be better than 20 fs (rms) by using a high-reliability femtosecond timing system developed for Linac Coherent Light Source (LCLS).<sup>12</sup> The electrons were generated by irradiating the photocathode with a femtosecond UV laser pulse at a 70° oblique incidence. The UV laser pulse was obtained by frequency tripling a small fraction of the output of the Ti:sapphire laser system which has a central wavelength of 800 nm, a maximum pulse energy of 3 mJ, and a pulse duration of 60 fs (FWHM). The majority (>70%) of the output of the Ti:sapphire laser system is delivered to the optical system for pumping the samples. The electron detector is located 3.2 m away from the sample and consists of a P43 phosphor

Note: Contributed paper, published as part of the Proceedings of the 21st Topical Conference on High-Temperature Plasma Diagnostics, Madison, Wisconsin, USA, June 2016.

<sup>a)</sup>Electronic mail: mmo09@slac.stanford.edu

screen ( $Gd_2O_2S:Eu$ ), a lens system, and a sensitive electron-multiplying CCD (EMCCD) camera (Andor iXon Ultra 888). In the middle of the phosphor screen there is a 1.6 mm diameter through hole to prevent the zero-order diffraction signal from saturating the CCD image at high EM gain during the experiments. A synchronized fast optical switch device consisted of two Pockels cells and a polarizer was installed before the compressor of the Ti:sapphire laser system to lower the laser repetition rate for single-shot operations. In this way, the high stabilities of the RF system can be maintained during single-shot data acquisition.

Fig. 1 shows the schematic diagram of the WDM experiment conducted with the MeV-UED system. The warm dense matter was created by irradiating a 130 fs (FWHM), 400 nm laser pulse at close to normal incidence onto a freestanding 35 nm-thick single-crystal gold foil. The gold nanofoils are mounted on an array of 350  $\mu\text{m}$  squared windows (pitched by 700  $\mu\text{m}$ ) of a silicon wafer, which can be motorized from outside the sample chamber. The 400 nm laser pulse was obtained through second harmonic generation of the principle wavelength via a 650  $\mu\text{m}$  thick  $\beta$ -barium borate crystal. The optical spot at the sample position has a diameter of  $\sim 420 \mu\text{m}$  with a quasi-flat-top spatial profile to ensure uniform heating of the sample. The flat-top profile was obtained by imaging the optical wavefront at a 4-mm-diameter iris located in the upstream onto the target with a  $f = 25 \text{ cm}$   $CaF_2$  lens. The pulse energy at target is adjustable and its maximum is  $\sim 300 \mu\text{J}$ .

The transmission electron diffraction for probing the warm dense gold was implemented with relativistic electrons with kinetic energy of 3.2 MeV. The focusing system for the electron beam is comprised of two separated solenoids and a collimator inserted in between. The collimator has three diameters, i.e., 100  $\mu\text{m}$ , 200  $\mu\text{m}$  and 500  $\mu\text{m}$ . During the experiment, the 200- $\mu\text{m}$ -diameter collimator was used to deliver an electron beam at the sample location with a satisfactory combination of the charge and the spot size. With this collimator, typical values of the charge and FWHM diameter of the optimized e-beam at sample were measured to be approximately 20 fC and 120  $\mu\text{m}$ , respectively. Fig. 2 shows the simulated spot size and pulse duration of the electron beam as a function of propagation distance as well as the measured spot sizes at the sample and detector locations. The simulation was done with the computer code, general particle tracer (GPT),<sup>13</sup> with typical experimental conditions. As indicated,

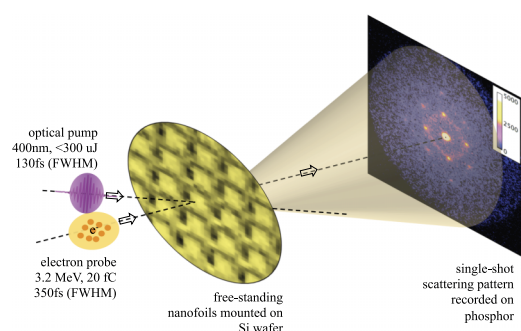


FIG. 1. Schematic diagram of the MeV UED pump-probe experiment for studying warm dense matter physics.

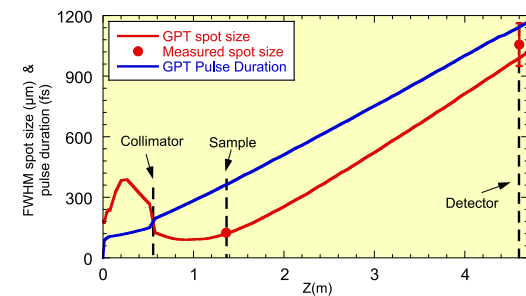


FIG. 2. GPT simulated FWHM spot size (red solid line) and FWHM pulse duration (blue solid line) of the 3.2 MeV electron beam propagating along the beamline. The horizontal axis plots the distance relative to the photocathode. Measured spot size of the electron beam at sample and detector locations are shown as red solid circles.

a good agreement in the spot size evolution is found between the simulation and the measurement. According to the GPT calculation, the pulse duration (FWHM) of the electron beam at the sample is predicted to be 350 fs. Assuming the temporal resolution of the pump-probe system is the quadratic combination of the pump pulse duration (130 fs), the probe pulse duration (350 fs) and the timing jitter between the two (20 fs), the temporal resolution is estimated to be approximately 370 fs FWHM, which is adequate to resolve the structural dynamics of the warm dense gold that takes place on picosecond time scales.<sup>5</sup>

### III. RESULTS AND DISCUSSIONS

Fig. 3 shows examples of the time-resolved single-shot UED patterns of the single-crystal gold pumped with 900 J/m<sup>2</sup> laser fluence. As indicated, high quality single-shot scattering images were obtained with the maximum scattering vector  $q$  defined by  $q = 2\pi \sin(\theta)/\lambda$  ( $\theta$ : scattering angle and  $\lambda$ : electron de Broglie wavelength) up to 11 Å<sup>-1</sup>. With this large  $q$  range, diffraction orders higher than (600) can be captured in a single-shot image. More importantly, a sufficiently high  $q$  range is essential to determine the pair correlation function of gold since the normalization between the measured scattering intensity and theoretical electron scattering factor is normally done at large  $q$ .<sup>14</sup> At time delay of 7 ps, the scattering image

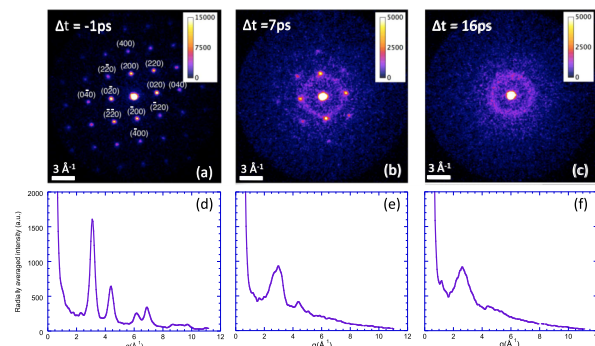


FIG. 3. (a)–(c) the single-shot UED patterns of the 35 nm freestanding single-crystal gold measured at different time delays relative to the arrival of the pump pulse, i.e., (a)  $-1 \text{ ps}$ , (b)  $7 \text{ ps}$ , and (c)  $16 \text{ ps}$ . The gold foil was excited by 400 nm laser pulse with pump fluence of 900 J/m<sup>2</sup>. Corresponding radially averaged lineouts of patterns ((a)–(c)) are shown from (d)–(f).

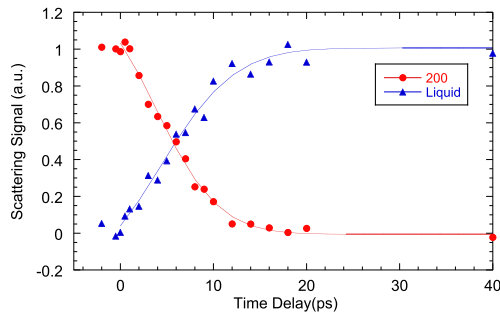


FIG. 4. Time dependence of the normalized (200) Bragg peak signal (red dots) and the scattering signal of the first liquid ring (blue triangles) as shown in the lineouts in Fig. 3. The solid lines are guide lines for the measured signals. Data at each delay point were determined from a single-shot measurement. The plotted Bragg signal is the sum of all the four equivalent peaks after background subtraction and the liquid signal is the sum of the signal between  $1.5 \text{ \AA}^{-1}$  and  $4 \text{ \AA}^{-1}$  of the radially averaged lineout of the four sectors not covered by the four (200) Bragg peaks.

shows the disappearance of the Bragg peaks with  $q$  positions above  $6 \text{ \AA}^{-1}$ , indicating the loss in the crystalline order. The broad scattering ring emerging nearby (200) Bragg peaks is an indication of the existence of the disordered liquid state, which contributes in part to the overall increase of the diffuse scattering background. At the longer delay of 16 ps, the measurement shows that the crystalline order is completely vanished and what remains is the highly disordered liquid state, which can be used to infer the dynamic liquid structure factors of WDM gold. Fig. 4 shows the single-shot measurement of the time dependence of Bragg peak (200) intensity as well as the liquid signal at the same pump fluence as in Fig. 3. As indicated, the trends of the Bragg peak decay and of the liquid signal raise are clearly observed by single shot measurement with this MeV UED system, allowing one to acquire high-quality data without averaging a large number of shots for statistics. The measured temporal behavior of the Bragg peak intensity and the liquid signal strength can then be used to test the theory of the structural dynamics and the melting mechanism of warm dense gold.<sup>5</sup>

#### IV. CONCLUSIONS

A single-shot MeV-UED apparatus has been developed to study the structural dynamics of warm dense matter. This

UED system takes advantage of the benefits of relativistic electrons as the probe source and is featured by high stability, high brightness, and femtosecond temporal resolution. The single-shot capability of this MeV-UED system was successfully demonstrated by probing the atomic structure changes of warm dense gold formed by optically pumping a 35 nm-thick freestanding single-crystal gold foil. The temporal evolution of Bragg peak intensity and the liquid signal of the melted gold were quantitatively determined with this MeV-UED system, opening up an exciting opportunity to unravel the atomic dynamics of laser-induced solid/liquid phase transitions in WDM regime.

#### ACKNOWLEDGMENTS

The authors would like to thank SLAC management for the strong support. The technical support by SLAC Accelerator Directorate, Technology Innovation Directorate, LCLS Laser Science & Technology Division and Test Facilities Department is gratefully acknowledged. This work was supported in part by the U.S. Department of Energy Contract No. DE-AC02-76SF00515, DOE Fusion Energy Sciences under FWP #100182, DOE BES Accelerator and Detector R&D program, and the SLAC UED/UEM Initiative Program Development Fund.

- <sup>1</sup>L. B. Fletcher *et al.*, *Nat. Photonics* **9**, 274 (2015).
- <sup>2</sup>P. Davis *et al.*, *Nat. Commun.* **7**, 11189 (2016).
- <sup>3</sup>N. Booth *et al.*, *Nat. Commun.* **6**, 8742 (2015).
- <sup>4</sup>J. D. Lindl, P. Amendt, R. L. Berger, S. G. Glendinning, S. H. Glenzer, S. W. Haan, R. L. Kauffman, O. L. Landen, and L. J. Suter, *Phys. Plasmas* **11**, 339 (2004).
- <sup>5</sup>R. Ernstorfer, M. Harb, C. T. Hebeisen, G. Sciaiani, T. Dartigalongue, and R. J. Dwayne Miller, *Science* **323**, 1033 (2009).
- <sup>6</sup>P. Musumeci, J. T. Moody, C. M. Scoby, M. S. Gutierrez, and M. Westfall, *Appl. Phys. Lett.* **97**, 063502 (2010).
- <sup>7</sup>B. J. Siwick, J. R. Dwyer, R. E. Jordan, and R. J. Dwayne Miller, *Science* **302**, 1382 (2003).
- <sup>8</sup>S. P. Weathersby *et al.*, *Rev. Sci. Instrum.* **86**, 073702 (2015).
- <sup>9</sup>R. Akre *et al.*, *Phys. Rev. Spec. Top. Accel. Beams* **11**, 030703 (2008).
- <sup>10</sup>B. Hong, R. Akre, and V. Pacak, in Proceedings of IPAC'10, Kyoto, Japan, 2010.
- <sup>11</sup>C. Rivetta, R. Akre, P. Cutino, J. Frisch, and K. Kotturi, in *Proceedings of PAC07* (IEEE, Albuquerque, NM, USA, 2007), p. MOPAS061.
- <sup>12</sup>K. Gumerlock *et al.*, Proceedings of FEL2014, Basel, Switzerland, 2014.
- <sup>13</sup><http://www.pulsar.nl/gpt/>.
- <sup>14</sup>B. J. Siwick, J. R. Dwyer, R. E. Jordan, and R. J. Dwayne Miller, *Chem. Phys.* **299**, 285 (2004).